Heliyon 10 (2024) e31509

Contents lists available at ScienceDirect

Heliyon

journal homepage: www.cell.com/heliyon

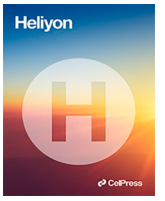

Research article

Inflammatory loop involving *Staphylococcus aureus*, IL-36γ, and cathepsin S drives immunity disorders in familial acne inversa keratinocytes

Yuanyuan Zhang [a,b], Weixue Jia [a], Xue Wang [a], Qiuxia Mao [c], Lingling Luo [a], Lingzhuo Kong [a], Youming Guo [a], Ran Mo [a], Wenbo Bu [d,*], Chengrang Li [a,**]

[a] *Hospital for Skin Diseases (Institute of Dermatology), Chinese Academy of Medical Sciences and Peking Union Medical College, Nanjing, Jiangsu, 210042, China*

[b] *Department of Dermatology and Venereology, Nanjing Drum Tower Hospital, Affiliated Hospital of Medical School, Nanjing University, Nanjing, Jiangsu, 210008, China*

[c] *Department of Dermatology, Jiangyin Hospital of Traditional Chinese Medicine, Jiangyin Hospital Affiliated to Nanjing University of Chinese Medicine, Jiangyin, Jiangsu, 214400, China*

[d] *Institute of Dermatology, Jiangsu Key Laboratory of Molecular Biology for Skin Diseases and STIs, Chinese Academy of Medical Science & Peking Union Medical College, Nanjing, Jiangsu, 210042, China*

A B S T R A C T

Acne inversa (AI) is an inflammatory skin disease associated with nicastrin (NCSTN) mutations. Despite the dysregulated bacterial–host immune interactions being an essential event in AI, the interaction between bacteria and keratinocytes in AI pathophysiology remains unclear. In this study, the NCSTN gene was suppressed using short hairpin RNA in HaCaT cells. Using RNA sequencing, real-time polymerase chain reaction, and western blotting, the expression of IL-36 cytokines was analyzed. The impact of *Staphylococcus aureus* on AI keratinocyte inflammation and underlying regulatory molecules was investigated by exposing the HaCaT cells to *S. aureus*. By stimulating NCSTN knockdown HaCaT cells with IFN-γ, the expression and regulatory mechanism of Cathepsin S (Cat S), an IL-36γ cleavage and activating protease, were investigated. After NCSTN knockdown, the IL-36α expression increased, and the IL-36Ra expression was downregulated. NCSTN/MEK/ERK impairment-induced Krüppel-like factor 4 (KLF4) up-regulation in concert with *S. aureus*-induced nuclear factor kappa B elevation acts synergistically to promote IL-36γ production with the subsequent IL-8 activation in HaCaT cells. NCSTN/MEK/ERK impairment was also observed in familial AI lesions. IFN-γ-induced Cat S in keratinocytes was enhanced after NCSTN knockdown. The expression of IFN-II pathway molecules was significantly upregulated in both NCSTN knockdown HaCaT cells and familial AI lesions. The Cat S expression was significantly elevated in the patient's AI lesions. Our findings suggested a synergistic relationship between *S. aureus* and NCSTN/MAPK/KLF4 axis in IL-36γ-induced familial AI keratinocytes.

1. Introduction

Acne inversa (AI) is a chronic, relapsing, inflammatory, follicular skin disease characterized by subcutaneous nodules and abscesses, with sinus and scar formation mostly in the apocrine gland-bearing regions. Treating AI is still challenging owing to its unknown etiology. Family history with autosomal dominant inheritance has been reported in patients with AI and is associated with mutations in the γ-secretase subunit, nicastrin (NCSTN), presenilin enhancer 2, and presenilin-1. Among them, the NCSTN gene has the highest mutation rate [1,2]. NCSTN exhibits anti-proliferative and pro-differentiation roles in keratinocytes, and functional loss

* Corresponding author.
** Corresponding author.
E-mail addresses: buwenbo@163.com (W. Bu), nylcr72@163.com (C. Li).

https://doi.org/10.1016/j.heliyon.2024.e31509
Received 24 November 2023; Received in revised form 13 May 2024; Accepted 16 May 2024
Available online 23 May 2024

mutations in NCSTN can stimulate keratinocyte proliferation and inhibit differentiation through activation of signaling pathways including mitogen-activated protein kinase (MAPK), NF-κB, Notch, and PI3K-AKT [3–6].

Hyperkeratosis and dysregulated differentiation of hair follicle epidermis leading to follicle blockage and rupture is suspected to participate in the AI pathogenesis, suggesting the role of dysregulated keratinocyte proliferation and differentiation in AI [7,8]. In addition, the interfollicular epidermal inflammation in the early stage of AI indicating that keratinocyte inflammation with dysregulated cytokines may also play an important role in AI pathogenesis [9,10]. Keratinocytes are the primary source of chemokines in response to external stimuli in the skin. During inflammation or immune responses, they synthesize various chemokines, with the expressed specific chemokines attracting corresponding types of immune cells to infiltrate the damaged skin areas [11]. The inflammatory cell infiltration within AI lesions includes neutrophils, lymphocytes, and macrophages, among which neutrophils are the predominant leukocytes, and neutrophil infiltration is a hallmark feature of AI skin lesions [12]. Activated neutrophils mediate AI skin damage through various mechanisms, including phagocytosis, degranulation, and the formation of neutrophil extracellular traps [13]. IL-8 and IL-36 are considered key cytokines produced by keratinocytes in AI pathogenesis, inducing neutrophil-mediated immune damage [14,15]. IL-8, a major chemokine for neutrophils, binds to its receptor CXCR1 on the surface of neutrophils, participating in their migration to AI sites [16]. In patients with AI, IL-8 expression is significantly upregulated at lesion sites, with elevated levels of the chemokine receptor CXCR1 on neutrophils, and the level of IL-8/CXCR1 correlates positively with the number of abscesses and nodules in patients with AI [17,18]. Studies have demonstrated that the expression of IL-8 in keratinocytes is regulated by IL-36γ [19,20]. The IL-36 subfamily (IL-36α, IL-36β, and IL-36γ) and the IL-36 receptor antagonist (IL-36Ra), belonging to the IL-1 family of cytokines, are primarily expressed in epithelial cells, especially keratinocytes, which are considered the key initiators of skin inflammation and are abnormally expressed in patients with AI [21–23]. Krüppel-like factor 4 (KLF4) has been demonstrated to promote the production of IL-36γ and is negatively regulated by the MAPK signaling pathway. The IL-36 promoter region contains two binding sites: a p65 binding site and an epidermal growth factor receptor inhibitor response element (EiRS), which respond to KLF4 and the NF-κB subunit p65, respectively [24]. Additionally, IL-36 can induce the production of other pro-inflammatory cytokines and its own expression in an autocrine manner [25,26].

Studies have reported arrays of bacterial specimens in AI lesions, such as *Staphylococcus aureus*, coagulase-negative *Staphylococcus*, and *Corynebacterium* species [27,28]. The efficacy of antibiotics in AI also indicates the participation of bacteria in AI pathogenesis [29]. *S. aureus* is the most common infectious microorganism in AI, colonizing in approximately 26 % of AI cases, and is associated with AI recurrence and antimicrobial resistance [30]. Moreover, bacteria have been hypothesized to play not only a primary infectious role but also a pathogenic role that aggravates the immune disorders in AI [31]. However, the related studies concerning the interaction between bacteria and keratinocytes in AI pathophysiology remain limited.

Thus, using the shRNA-mediated gene knockdown and RNA sequencing technology, we explored the differentially expressed signaling pathways regulated by NCSTN deficiency. Through exposing NCSTN knockdown HaCaT cells *to S. aureus*, we investigated the impact of S. aureus on keratinocyte inflammation and the related immune mechanisms in AI, and explored the activation mechanism of related molecules in AI.

2. Materials and methods

2.1. Human tissue specimen

A Chinese Han family comprising four related patients with AI was first diagnosed at our institution in 2018. After obtaining written informed consent from all the patients, we obtained clinical data and lesion skin tissues of the four patients. We also collected AI skin lesions from eight sporadic patients as well as normal skin tissues from four healthy controls, among which the normal skin tissue biopsy samples were obtained from the four healthy individuals undergoing dermatoplastic surgery at our institution. This study was authorized by the Ethics Committee of Hospital for Skin Diseases (Institute of Dermatology), Chinese Academy of Medical Sciences, and Peking Union Medical College and was conducted in accordance with the Declaration of Helsinki (approval number: 2021-KY-056).

2.2. Cell culture

Human keratinocyte cell line HaCaT was purchased from National Collection of Authenticated Cell Cultures (Chinese Academy of Sciences, Shanghai, China) and cultured in Dulbecco's modified Eagle's medium (Lonza, Walkersville, MD, USA) supplemented with 10 % bovine pituitary extract (Thermo Fisher Scientific, Waltham, MA, USA) and 1 % antibiotics (100 μg/mL streptomycin and 100 U/mL penicillin) at 37 °C and 5 % CO2.

2.3. NCSTN knockdown HaCaT cell model

The HaCaT cells were infected with the lentivirus particles containing scrambled control shRNA (negative control group, NC group) and NCSTN targeting shRNA (interference group, shRNA group). The lentivirus particles containing shRNA were from GenePharma (Shanghai, China), and the shRNA sequence is listed in Supplementary Table S1. After 72 h of transfection, shRNA-expressing cells were selected using 2 mg/L puromycin for 5 d, and then RNA and protein were extracted.

2.4. Sequencing

Total RNA was extracted from 3 shRNA and 3 NC groups HaCaT cells, respectively, with Trizol and quality controlled on the purity, concentration, and integrity. The mRNA carrying 3′-poly (A) tails were enriched with Oligo (dT) magnetic beads and fragmented in NEB fragmentation buffer. Subsequently, first- and second-strand cDNA were synthesized in the M-MuLV reverse transcriptase system and the DNA polymerase I system, respectively. The purified double-stranded cDNA was ligated using the NEBNext adaptor. After polymerase chain reaction (PCR) amplification and purification with AMPure XP beads, the libraries were established and sequenced on the Illumina HiSeq platform at the Novogene Bioinformatics Institute (Beijing, China).

2.5. Differential expression analysis

The DESeq R package (GitHub, San Francisco, CA, USA) was adopted to conduct a differential expression analysis [32]. For controlling the false discovery rate, P-values were adjusted with the Benjamini and Hochberg's approach. Genes with adjusted P (padj) value < 0.05 were considered differentially expressed. The KOBAS software (Peking University, Beijing, China) was used to explore the Kyoto Encyclopedia of Genes and Genomes (KEGG) pathways enriched by differentially expressed genes (DEGs) [33]. $P < 0.05$ in the hypergeometric test was considered significant. RNA-seq data were submitted to the GEO database (accession number: GSE209911).

2.6. Quantitative real-time reverse transcriptase PCR (qRT-PCR) validation

Total RNA was extracted with Trizol. After the concentration and purity were qualified, the RNA was reverse transcribed into cDNA (Takara Bio, Otsu, Japan). Then, 20 μL of mix: water, cDNA, primers (Life Technologies, Shanghai, China). SYBR Green Taq (Takara Bio, Otsu, Japan) was reacted in the FastStart Universal SYBR Green Master (ROX) system. The reaction conditions were as follows: denaturation step of 30 s at 95 °C, followed by 40 cycles at 95 °C for 5 s, and 60 °C for 20 s, and 65 °C for 15 s. The CT value was relatively quantified using the $2^{-\triangle\triangle}$CT method. The primer sequences are listed in Supplementary Table S2.

2.7. Western blot (WB) analysis

WB was performed as previously described [34]. Briefly, proteins were extracted by lysing cells with radioimmunoprecipitation assay buffer (Beyotime, Nantong, China), followed by quantification of protein concentrations using the bicinchoninic acid protein assay kit (P0010, Beyotime, Nantong, China). Subsequently, 60 μg of protein per sample was resolved by sodium dodecyl-sulfate polyacrylamide gel electrophoresis (Beyotime, Nantong, China) and transferred onto nitrocellulose membranes (Gelman Laboratory, Ann Arbor, MI, USA). These membranes were then blocked using 5 % bovine serum albumin (BSA) (Beyotime, Nantong, China) for 1 h before incubation with respective primary antibodies at 4 °C overnight. On the next day, the membranes were treated with secondary antibodies at room temperature for 1 h. Following several washes, the blots were visualized using enhanced chemiluminescence detection reagent (Merck Millipore, Hayward, CA, USA) and the FluorChem E fluorescence band detection system (Genentech, South San Francisco, CA, USA). For blot analysis, the procedure included adjusting images to an 8-bit format and selecting the relevant bands, generating plot lanes and demarcating groups with lines at the base, and measuring the area of each band. The intensity of the bands was quantified using the Image J software (National Institutes of Health, Bethesda, MD, USA). The antibodies are listed in Supplementary Table S3.

2.8. Immunofluorescence

Following deparaffinization and rehydration as described above, skin tissue sections were processed for epitope retrieval by heating the slides in ethylenediaminetetraacetic acid (EDTA) antigen retrieval buffer at a pH of 8.0 (Beyotime, Nantong, China) using a microwave. The sections were then permeabilized with Clear Solution (Beyotime, Nantong, China) and blocked using 3 % BSA (Beyotime, Nantong, China). Primary antibodies were applied to the sections and left to bind for 12 h at 4 °C. Following primary antibody incubation, the sections were rinsed with phosphate-buffered saline (PBS) and incubated with Alexa-647-labeled secondary antibody (Thermo Fisher Scientific, Waltham, MA, USA) for 30 min at room temperature. Nuclei staining was achieved by counterstaining the samples with 4′,6-diamidino-2-phenylindole. Immunofluorescent images were obtained and documented using an Olympus BX53 confocal microscope (Olympus Corporation, Tokyo, Japan) at 200 × magnification. The antibodies are listed in Supplementary Table S3.

2.9. Immunohistochemistry

Skin tissue sections, embedded in paraffin and cut to a thickness of 4–5 μm, were affixed to poly-L-lysine-coated slides and incubated at 37 °C overnight to ensure proper adhesion. Subsequently, the sections underwent deparaffinization through a series of treatments with xylene and alcohols to eliminate paraffin and prepare the tissues for staining. Antigen was then retrieved using Tris-EDTA buffer (pH 6) in a microwave, followed by cooling and rinsing. To inhibit endogenous peroxidase activity, the sections were treated with 3 % hydrogen peroxide in methanol, and then blocked with serum. Prepared primary antibodies were applied to the tissue sections for 12 h at 4 °C to facilitate binding. After washing with PBS, secondary antibodies were applied for 30 min at room temperature. Target proteins were visualized by adding a peroxidase substrate (DAB) (Beyotime, Nantong, China) for 5 min. The sections

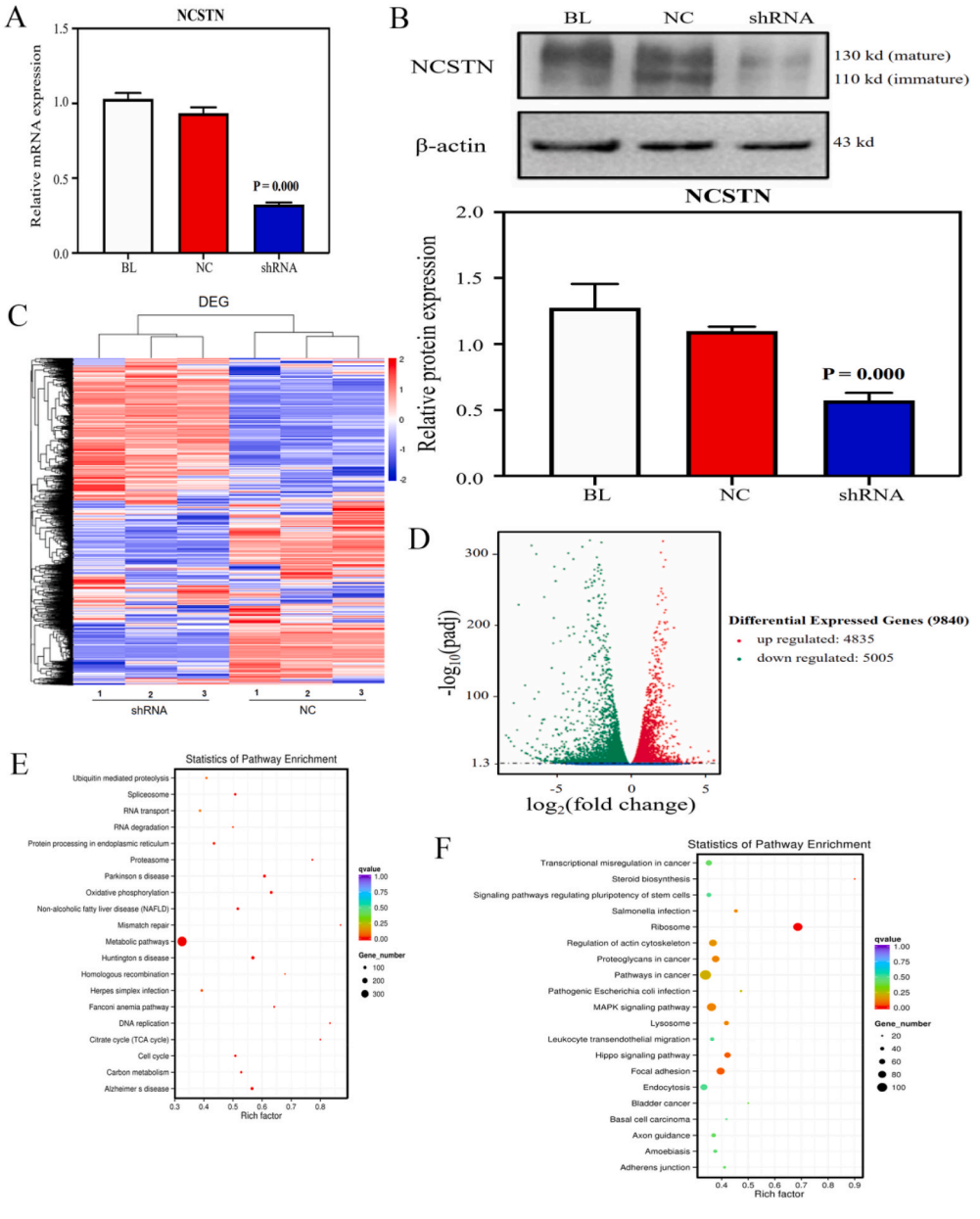

(caption on next page)

Fig. 1. Differentially expressed genes (DEGs) after nicastrin (NCSTN) deficiency in HaCaT cells.
NCSTN expression revealed by quantitative real-time reverse transcriptase polymerase chain reaction (qRT-PCR) (A) and Western blot (B) in the HaCaT cells of the BL group (uninfected), NC group (infected with shNC lentiviral vectors), and shRNA group (infected with sh-NCSTN lentiviral vectors). The NCSTN protein exists in two forms: immature (imNCT) and mature (mNCT). The heatmap (C) and volcano plot (D) displays the DEGs in NCSTN knockdown HaCaT cells measured by RNA sequencing. The TOP 20 most enriched KEGG pathways by upregulated (E) and downregulated (F) DEGs. Rich factor refers to the ratio of the number of DEGs involved in the pathway to all genes involved in the pathway. The Q value is the corrected *P* value by multiple hypothesis testing, the closer to zero, the more significant the enrichment. (G) Validation of the MKI67, TGFβ2, MEK1/2, ERK1/2, and RAF in NCSTN knockdown HaCaT cells by quantitative real-time reverse transcriptase polymerase chain reaction. Results are expressed as means ± standard deviations (n = 3).

were then mounted under coverslips for microscopic examination and photographed using an Olympus CX23 light microscope (Olympus Corporation, Tokyo, Japan) at magnifications of 100 × or 200 × . The antibodies are listed in Supplementary Table S3.

2.10. Enzyme-linked immunosorbent assay (ELISA)

The IL-8 ELISA kits (R&D Systems, Minneapolis, MN, USA) were utilized to measure the IL-8 levels secreted by HaCaT cells. Initially, IL-8 capture antibodies were coated onto 96-well microplates to create a solid-phase antibody base. Following *S. aureus* stimulation, HaCaT cell culture medium was collected and centrifuged at 1000 g and 4 °C for 10 min to remove cellular debris. Subsequently, 40 μL of diluent and 10 μL of the supernatant containing IL-8 were transferred into the enzyme-labeled coating microplate and incubated for 30 min at 37 °C. After washing the microplate five times, it was incubated with an enzyme-linked polyclonal IL-8 antibody for 30 min at 37 °C. Following a repeat of the washing steps, 3,3′,5,5′-tetramethylbenzidine substrate was added to the wells. The reaction was halted by adding a stop solution, and the absorbance was measured at 450 nm using the Multiskan FC Microplate Photometer (Thermo Fisher Scientific, Waltham, MA, USA).

2.11. Statistical analysis

All statistical data were analyzed using the SPSS 17.0 software (SPSS Software, CA, USA). The results are expressed as means ± standard errors. The differences between the two groups were evaluated using the Student's t-test. All experiments were performed in triplicate, and significance was set at $P < 0.05$.

3. Results

3.1. Transcriptomic profile of NCSTN knockdown HaCaT cells

Initially, we built the NCSTN-shRNA-knockdown HaCaT cell model. Compared with the NC group, the NCSTN expression in the interference group (shRNA group) was significantly downregulated at the mRNA ($P < 0.001$) and protein ($P < 0.001$) levels (Fig. 1A and B).

The transcriptomes of NCSTN knockdown HaCaT cells were measured by RNA sequencing (Fig. 1C). A total of 9840 mRNAs were identified as DEGs between the shRNA and the NC group (Fig. 1D). MKI67 (2.50 Log2 fold change) and transforming growth factor-beta 2 (TGFB2) (−5.61 Log2 fold change) were the most significantly upregulated and downregulated DEGs, respectively (Supplementary Table S4). The KEGG pathway analysis revealed the signaling pathways enriched by DEGs (Fig. 1E and F), and the MAPK signaling pathways were one of the most downregulated pathways (Fig. 1F). We also observed a significant down-regulation of NF-κB and the Notch signaling pathway in the sequencing data (Supplementary Table S4).

Furthermore, we validated the MKI67 and TGFB2 and MAPK pathway molecules using qRT-PCR. Compared with the NC group, the MKI67 expression ($P = 0.006$) was significantly upregulated, whereas the TGFB2 ($P = 0.010$), extracellular signal-regulated kinase (ERK1/2) ($P = 0.026$), MAPK/ERK kinase (MEK1/2) ($P = 0.042$), and RAF ($P = 0.012$) were significantly downregulated, which was consistent with the expression level obtained from the sequencing analyses (Fig. 1G).

3.2. IL-36 up-regulation in NCSTN knockdown HaCaT cells

NCSTN is a key pathogenic gene in AI, and IL-36 is a key initiator of skin inflammation. To explore the relationship between NCSTN in AI pathogenesis and the initiation of inflammation, we examined the expression of the IL-36 family in NCSTN knockdown HaCaT cells. Changes in IL-36 expression were observed following NCSTN knockdown, as evidenced in the sequencing results (Supplementary Table S4). Therefore, we verified the IL-36 cytokines level using qRT-PCR and WB to explore the effect of NCSTN knockdown on keratinocyte inflammation. The IL-36α expression increased ($P = 0.001$), and whereas the IL-36Ra expression was downregulated ($P < 0.001$) after NCSTN knockdown. However, no significant change was observed in IL-36β and IL-36γ levels (Fig. 2A and B). These results suggest that NCSTN knockdown induces dysregulation of IL-36 expression in HaCaT cells, thereby initiating inflammation.

3.3. IL-36γ induced by NCSTN/MAPK/KLF4 axis and S. aureus-induced NF-κB elevation

Although S. aureus is the primary contaminating microorganism causing AI, its specific role in modulating cytokine secretion by

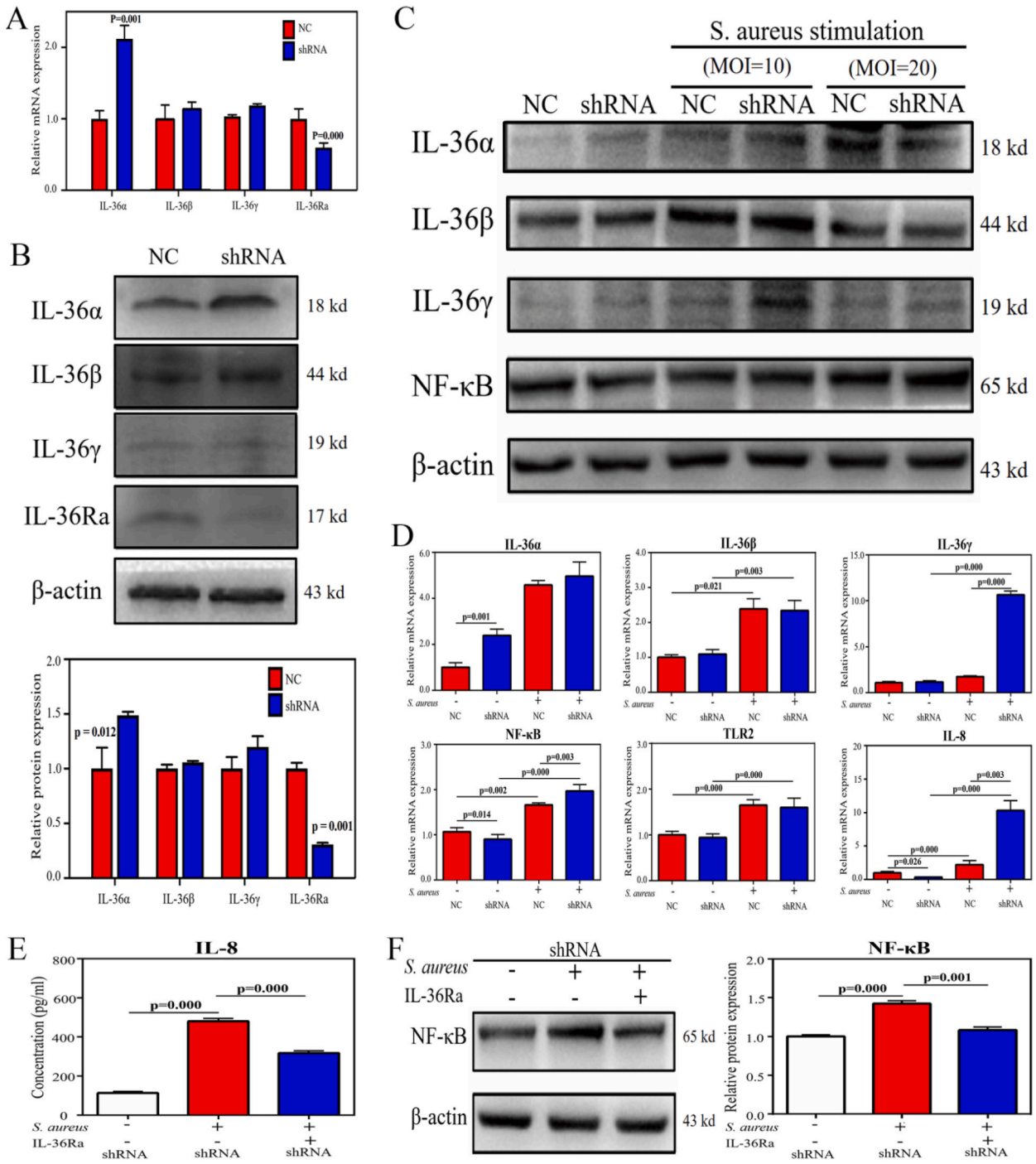

Fig. 2. Increased IL-36γ expression in nicastrin knockdown HaCaT cells stimulated with *Staphylococcus aureus*.
The IL-36 subfamily (IL-36α, IL-36β, and IL-36γ) and IL-36 receptor antagonist (IL-36Ra) expression level were validated by quantitative real-time reverse transcriptase polymerase chain reaction (qRT-PCR) (A) and western blotting (B) of HaCaT cells in the NC and shRNA groups. *S. aureus* cells were collected, and their concentration was measured with a microplate reader. The cells were diluted with serum-free Dulbecco's modified Eagle's medium. (C) The HaCaT cells of the NC and shRNA groups were exposed to *S. aureus* (MOI 10 and 20) for 8 h. The expression in protein level of IL-36 cytokines, TLR, IL-8, and NF-kB were analyzed by western blotting. (D) The HaCaT cells of the NC and shRNA groups were exposed to *S. aureus* (MOI 10) for 8 h. The expression of IL-36 cytokines, TLR2, IL-8, and NF-kB were analyzed by qRT-PCR. IL-36Ra (1 μg/mL) can significantly reduce (E) the secretion of IL-8 and (F) expression of NF-κB under the stimulation of *S. aureus*, detected by enzyme-linked immunosorbent assay and western blotting, respectively. Results are expressed as means ± standard deviations (n = 3).

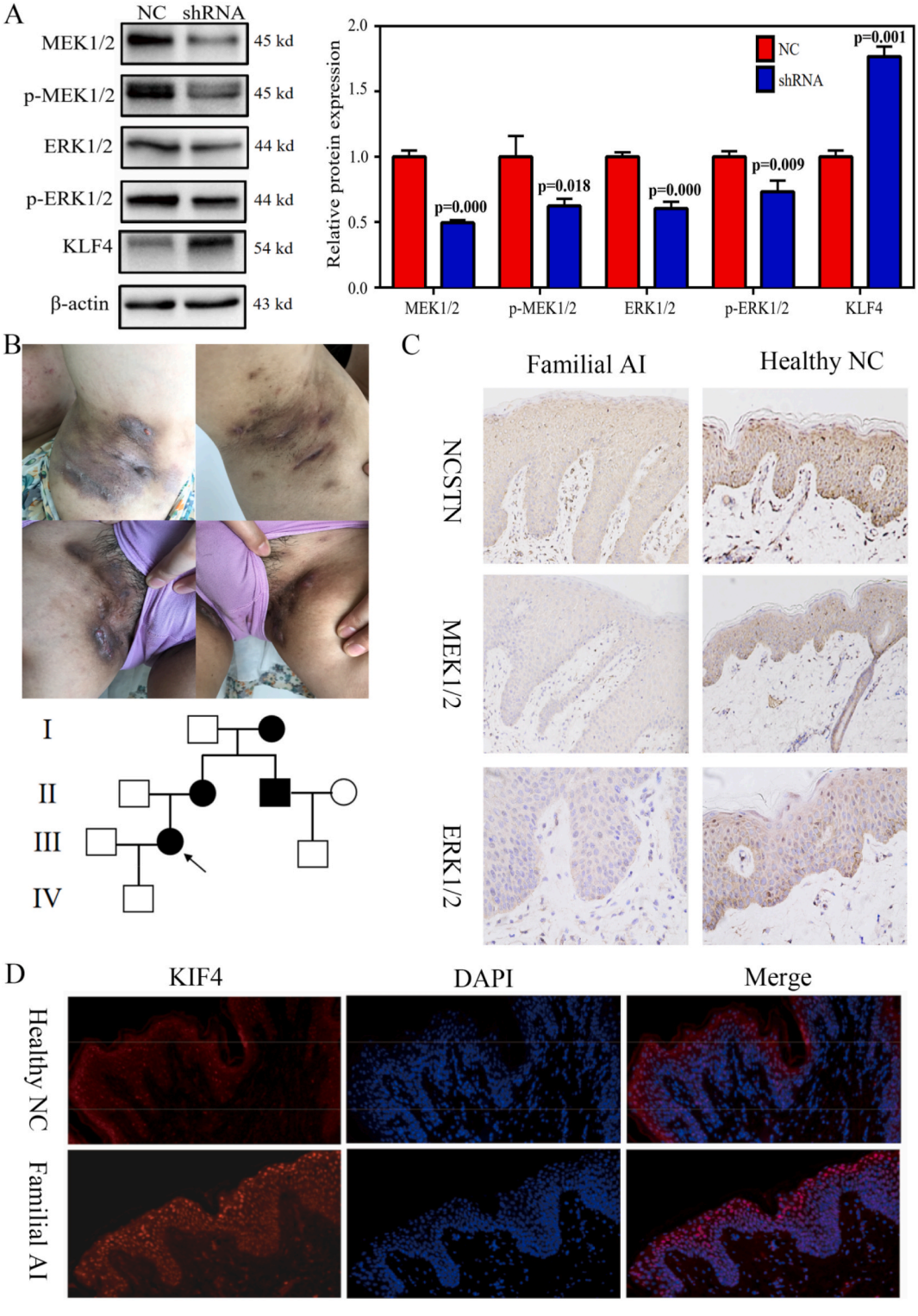

(caption on next page)

Fig. 3. Altered MEK/ERK/KLF4 axis in nicastrin (NCSTN) knockdown HaCaT cells and the NCSTN/MEK/ERK deficiency in familial AI patient lesion.
(A) The expression levels of MAPK signaling pathway molecules (ERK1/2, *p*-ERK1/2, MEK1/2, and *p*-MEK1/2) and downstream KLF4 were analyzed by western blotting in NCSTN knockdown HaCaT cells. (B) Painful subcutaneous nodules, abscesses, sinus, and scars in the axillary and groin area of the proband and the family tree reveal the affected individuals in the AI family. (C) Immunohistochemistry revealed the NCSTN, MEK1/2, ERK1/2 expression levels in the proband patient of a Chinese AI family. Original magnification × 100 (NCSTN, MEK1/2); × 200 (ERK1/2). (D) Immunofluorescence revealed the KLF4 expression in the epidermis of familial AI lesions (original magnification × 200). Results are expressed as means ± standard deviations (n = 3).

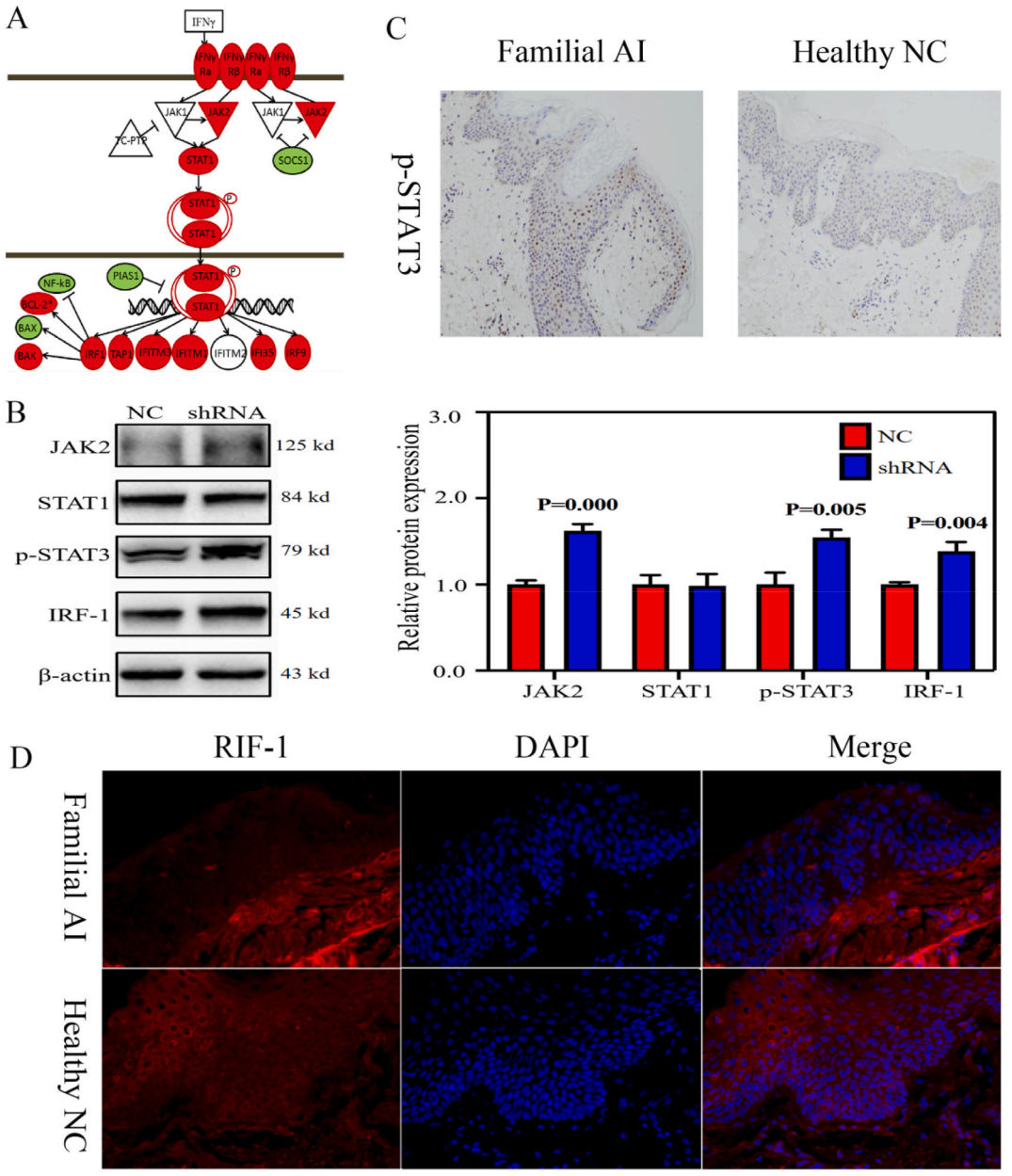

Fig. 4. Altered type II IFN signaling in nicastrin (NCSTN) knockdown HaCaT cells and familial AI patient lesion.
(A) The upregulated IFN-II pathway in the sequencing results of NCSTN knockdown HaCaT cells. Upregulated gene nodes are marked in red, downregulated gene nodes are marked in green, and unmarked nodes have no significant difference. (B) Western blotting revealed the expression of IFN-II pathway molecules (JAK2, STAT1, p-STAT3 and IRF1) in NCSTN knockdown HaCaT cells. The P-STAT3 (C) and IRF-1 (D) expressions in the epidermis of the proband patient lesion of a Chinese AI family revealed by immunohistochemistry and immunofluorescence, respectively. Original magnification × 200.

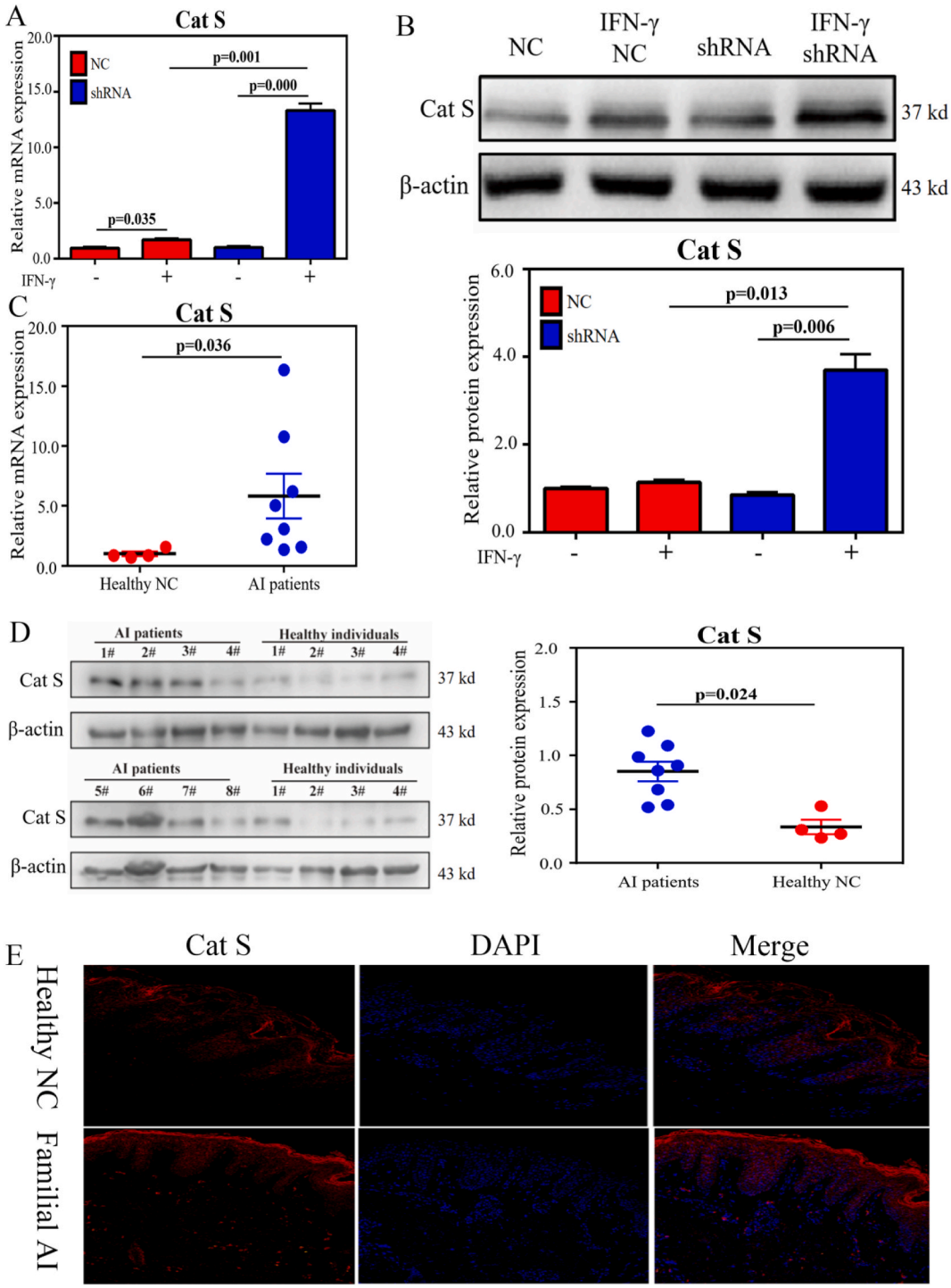

Fig. 5. Enhanced IFN-γ-induced up-regulation of Cat S in nicastrin knockdown HaCaT cells, and the elevated expression of Cat S in the skin lesions of patients with AI.

The HaCaT cells of the NC and shRNA groups were stimulated with 200 ng IFN-γ for 48 h. The expression level of Cat S was measured using quantitative real-time reverse transcriptase polymerase chain reaction (qRT-PCR) (A) and western blotting (B). The Cat S expression levels of AI skin lesions and normal skin tissues (8 AI patients; 4 healthy individuals) were measured using qRT-PCR (C), Western blot analysis (D) and immunofluorescence (E), respectively. Original magnification × 200. Results are expressed as means ± standard deviations (n = 3).

keratinocytes has not been thoroughly investigated. Hence, we exposed the HaCaT cells to *S. aureus* (ATCC, USA, Cat#25923) (MOI 10 and 20) for 8 h to observe the IL-36 cytokine expression. The expression of IL-36α ($P = 0.001$), IL-36β ($P = 0.003$), IL-36γ ($P < 0.001$), and Toll-like receptor 2 (TLR2) ($P < 0.001$) are significantly increased by exposure to *S. aureus* both in the shRNA and NC groups (Fig. 2C and D). Interestingly, the IL-36γ expression was significantly enhanced in shRNA group at the mRNA and protein levels (Fig. 2C and D). However, no significant differences of the IL-36α, IL-36β, and TLR2 expression were observed between the NC and shRNA groups (Fig. 2C and D).

The original expression of NF-κB ($P < 0.001$) and IL-8 ($P < 0.001$) in the shRNA group was significantly lower than that in the NC group (Fig. 2C and D), which might be attributed to the down-regulation of the Notch pathway caused by NCSTN knockdown. However, after *S. aureus* stimulation, the NF-κB ($P = 0.006$) and IL-8 ($P = 0.012$) expression significantly increased both in shRNA and NC group. It is noteworthy that the NF-κB ($P = 0.002$) and IL-8 ($P < 0.001$) up-regulation was significantly enhanced in NCSTN knockdown HaCaT cells (Fig. 2C and D). Furthermore, the natural IL-36 inhibitor, recombinant IL-36Ra (Novoprotein, Suzhou, China) addition can significantly decrease the IL-8 ($P < 0.001$), and NF-κB ($P < 0.001$) expression (Fig. 2E and F). These results suggested that *S. aureus* stimulation in NCSTN knockdown HaCaT cells drove elevated IL-36γ expression with subsequent activation NF-κB and the neutrophil chemotactic factor IL-8.

Considering the involvement of the MAPK pathway in the pathogenesis of AI and the production of IL-36γ, we also focused on the expression of MAPK in NCSTN knockdown HaCaT cells. The sequencing data of NCSTN knockdown HaCaT cells revealed the significant down-regulation of the MAPK signaling pathway (Fig. 1E and F). Fig. 3A demonstrated significant down-regulation of ERK1/2 ($P < 0.001$), MEK1/2 ($P < 0.001$), phosphorylation ERK (*p*-ERK1/2) ($P = 0.009$), and *p*-MEK1/2 ($P = 0.018$) in NCSTN knockdown HaCaT cells. Moreover, we also identified a significant down-regulation of NCSTN ($P = 0.007$), ERK1/2 ($P = 0.035$), and MEK1/2 ($P = 0.012$) in the lesions of the proband in a Chinese AI family with four affected individuals (Fig. 3B and C).

Furthermore, we observed an enhanced KLF4 expression ($P < 0.001$) in NCSTN knockdown HaCaT cells (Fig. 3A), which has been demonstrated to promote the IL-36γ production and is negatively regulated by MAPK signaling. Immunofluorescence revealed that compared with the normal skin tissues, the KLF4 expression was elevated in the epidermis of the lesions of patients with familial AI (Fig. 3D). Two binding sites: p65 binding site and EiRS exist in the promoter region of IL-36, which respond to KLF4 and NF-κB subunit p65 respectively. We observed a significant down-regulation in NF-κB signaling after NCSTN knockdown (Fig. 2C and D); therefore, the increased KLF4 expression led by NCSTN/MAPK impairment might not effectively induce the IL-36γ expression. *S. aureus* stimulation of keratinocytes activated the NF-κB signaling pathway (Fig. 2C and D), which may have partnered with upregulated KLF4 to enhance the IL-36γ secretion in NCSTN knockdown HaCaT cells.

These data demonstrated that NCSTN/MAPK/KLF4 signaling pathway and S. aureus-induced NF-κB elevation act synergistically to induce IL-36γ production with subsequent activation of NF-κB and the neutrophil chemotactic factor IL-8 in AI keratinocytes.

Upregulated type II IFN signaling promoted Cathepsin S (Cat S) secretion upon IFN-γ stimulation in NCSTN knockdown HaCaT cells.

IL-36γ is expressed as an inactive precursor, requiring activation through proteolytic processing by proteases such as Cat S, which are secreted by keratinocytes via the IFN-γ and interferon regulatory factor (IRF-1) pathways. In sequencing data, we observed that the IFN-II pathway was elevated upon NCSTN knockdown in HaCaT cells (Fig. 4A). In addition, the expression of Janus kinase 2 (JAK2) ($P < 0.001$), phospho-STAT3 (p-STAT3) ($P = 0.005$), and IRF-1 ($P = 0.004$) were verified to significantly increase in NCSTN knockdown HaCaT cells (Fig. 4B). In addition, we also observed significantly elevated p-STAT3 ($P = 0.031$) and IRF-1 ($P < 0.001$) expression levels in the epidermis of patients with familial AI lesions (Fig. 4C and D).

We stimulated NC and NCSTN-knockdown HaCaT cells with 200 ng IFN-γ (PeproTech, USA) to explore the regulation of IFN-γ on AI keratinocyte Cat S secretion. After 48 h, the Cat S expression was measured. Despite no significant difference in the Cat S expression between the shRNA and NC groups, the Cat S expression level ($P = 0.001$) in the IFN-γ-stimulated NCSTN-shRNA group was significantly higher than that in the IFN-γ-stimulated NC group (Fig. 5A–C).

These results demonstrated that the upregulated IFN-II signaling pathway after NCSTN knockdown in keratinocytes increased the keratinocyte Cat S secretion under the IFN-γ stimulation.

3.4. Cat S up-regulation in AI lesions

Considering the crucial role of Cat S in the activation of IL-36, we examined the expression of Cat S in AI lesions in clinical samples. With the approval of the local medical ethical committee and the informed patient's consent, biopsies were performed in eight patients with AI diagnosed based on criteria and four healthy individuals undergoing cosmetic surgery procedures. The Cat S expression in skin lesions of patients with AI and normal skin tissues were measured using qRT-PCR and WB analyses. The Cat S expression ($P = 0.024$) was significantly elevated in the skin lesions of patients with AI compared with normal skin tissues (Fig. 5D–E). The over-secreted Cat S might contribute to the cleavage and activation of IL-36γ with subsequent induction of the neutrophil chemotactic factor IL-8 in AI lesions.

4. Discussion

This study demonstrated that NCSTN/MAPK impairment partnered with *S. aureus*-induced keratinocyte IL-36γ expression. The upregulated IFN-II signaling pathway after NCSTN knockdown in keratinocytes increased the IFN-γ-induced Cat S secretion, thereby contributing to the cleavage and activation of IL-36γ and driving IL-8-mediated neutrophil enrichment inflammation in AI.

The IL-36α expression elevation after NCSTN knockdown was consistent with a previous finding that NCSTN knockout increased

the IL-36α expression in mouse epidermis [35]. IL-36Ra deficiency was identified in several pustular skin diseases and has been considered a key molecule of autoinflammatory keratinization diseases [36]. IL-36α, IL-36β, and IL-36γ were upregulated in AI both systemically and lesionally. However, as a natural receptor antagonist of IL-36, IL-36Ra was reported to be not significantly expressed in AI lesions [37–39]. The imbalance of IL-36/IL-36RA might induce and accelerate an immune disorder in AI lesions.

The clinical signs in active AI, the bacterial species identified from AI lesions, and the positive response to antibiotics in patients with AI strongly indicate the role of bacteria in AI pathogenesis. However, the related mechanism of bacteria in AI pathogenesis remains unclear. Rather than as classic infectious pathogens, bacteria have been hypothesized to be activators of the disordered bacterial–host immunity interactions of AI [27–29]. Studies reflected the hyperactive systemic immune response to bacteria and the impaired antibacterial ability in patients with AI, concerning IL-26, IL-1β, IL-6, IL-23, IL-17α, and β-defensin [40]. Besides, the IL-22 and AMP deficiency in AI lesions revealed weak epidermal antimicrobial defense in AI, leading to increased frequency of skin infections in patients [41]. However, the related studies concerning the interaction between bacteria and keratinocytes in the pathophysiology of AI are still limited. We observed that MEK/ERK was downregulated after NCSTN knockdown, leading to the up-regulation of downstream KLF4 expression. KLF4 was reported to play an essential role in terminal epidermal cell differentiation [42,43]. The NCSTN/MAPK/KLF4 axis contributes to epidermal differentiation dysregulation, which may contribute to the epidermal barrier dysfunction and follicular occlusion, thus promoting bacterial invasion in AI. Meanwhile, the NCSTN/MAPK/KLF4 axis partners with bacteria factors to induce an elevation of IL-36γ with subsequent activation of NF-κB and IL-8 in keratinocytes, leading to neutrophil enrichment inflammation in AI (Fig. 6). This may be relevant to the special area features of AI lesions. These areas (apocrine gland-bearing areas: axillary, inguinal, and anogenital regions; intertriginous areas that do not bear apocrine glands: submammary fold) are subject to skin friction. Moreover, the high temperature and moisture in these areas also favor specific microbiome multiplication.

Our results revealed that Cat S expression was elevated in AI lesions. As reported, IL-36γ can be activated by neutrophil proteases, and then induce keratinocyte neutrophil chemokine production [44]. However, in perilesional and early-stage AI skin lesions, lymphocytes are the dominant infiltrating cells, while neutrophils mainly infiltrate the deep dermal lesions and play a role in the later stages of the inflammatory process [8,9]. Cat S precisely cleaved IL-36γ, and the cleavage product of IL-36γ was Ser18 which induced hyperkeratosis and epidermal psoriasiform changes in the human skin model, which is consistent with the early pathological characteristics of AI [45]. Cat S is expressed in the skin-resident cells, including fibroblasts and keratinocytes, and remains bioactive in the neutral extracellular environments [46]. Compared with the neutrophil proteases that need cellular recruitment and degranulation, the upregulated Cat S expression in AI lesions may have a more dominant role for IL-36γ cleaving and activating in the early stage of

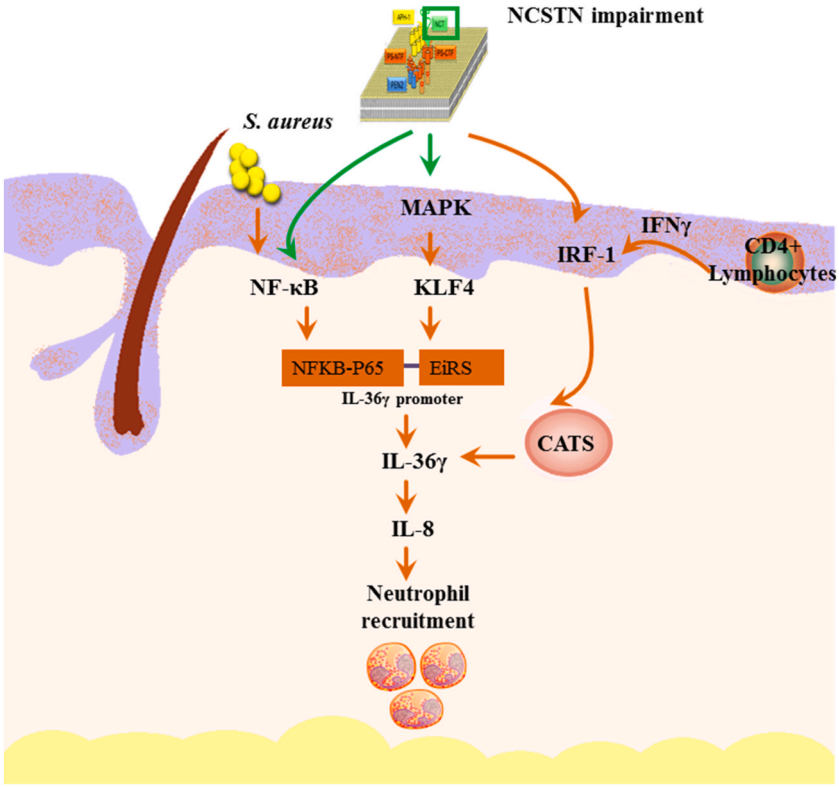

Fig. 6. Model for the synergistic relationship between *Staphylococcus aureus*-induced NF-κB elevation and NCSTN/MAPK/KLF4 signaling pathway in the pathophysiology of acne inversa (AI), and the overexpression mechanism of Cat S in AI epidermis. The green arrow represents down-regulation, whereas the red arrow represents up-regulation.

the disease [39].

The enhanced IFN-γ-induced up-regulation of Cat S is associated with the upregulated IFN-II pathway in NCSTN-knockdown HaCaT cells. Moreover, the elevated IFN-II pathway after NCSTN deficiency may be a theoretical basis for the potential effectiveness of JAK inhibitors in AI [47]. In the IFN-II pathway, IRF1 is a transcriptional mediator of IFN-γ-dependent Cat S activation; IRF1 overexpression increased the IFN-γ-induced Cat S expression in epithelial cells [48]. The IRF-1 expression was also elevated in the transcriptome data of AI lesions [49]. In addition, the perilesional and lesional skins of patients with AI were characterized by the infiltration of $CD4^+$ T cells that secreted IFN-γ [50]. The increased IRF-1 expression might further amplify the effect of elevated IFN-γ in AI lesions, promote Cat S expression, and activate $CD4^+$ T cells and IL-36γ subsequently [45]. The IFN-II pathway and Cat S may play an essential role in the interaction between T cells and keratinocytes and form an inflammatory loop, which aggravates the AI immune disorder.

Our findings suggested a synergistic relationship between microbial factors and keratinocyte immunity in the AI physiopathology. Further experiments are needed to explore the precise regulatory mechanism of MAPK and IFN-II pathway in AI. However, which specific components of *S. aureus* contribute to this process is not clear; since some studies [51] have reported the absence of *S. aureus* in certain AI patient cohorts, other microbes could play a similar role in AI through the same pathways. Moreover, the study's limitation is its in vitro nature, which limits the direct applicability of the findings to in vivo conditions. Future studies should validate these mechanisms in clinical studies and evaluate the therapeutic effects of targeting the NCSTN/MAPK/KLF4 axis in patients with AI. Targeting IL-36 therapies such as anti-IL-36 receptor antibody under phase II clinical trials in patients with palmoplantar pustulosis or generalized pustular psoriasis, may also have a possibility for targeted therapy in AI [52,53]. Our results also suggest the possibility of therapeutic targeting Cat S through Cat S inhibitors in AI treatment.

5. Conclusion

This study elucidates the pathophysiological mechanisms in AI linked to NCSTN mutation through in vitro experiments and validation with clinical samples, highlighting a synergistic effect between *S. aureus* and the NCSTN/MAPK/KLF4 axis on IL-36γ induction. The findings offer insights into the *S. aureus*–host interactions and potential targets for therapeutic intervention in AI.

Funding

This project is supported by the Natural Science Foundation of China (81472872), the Natural Science Foundation of Jiangsu Province (BK20211027), the central universities fundamental research funds in PUMC (3332019160) and CAMS Innovation Fund for Medical Sciences (2021-1-I2M-018, 2021-I2M-1-001).

Ethics declarations

This study was reviewed and approved by the Ethics Committee of Hospital for Skin Diseases (Institute of Dermatology), Chinese Academy of Medical Sciences and Peking Union Medical College, with the approval number: 2021-KY-056.

All participants provided informed consent to participate in the study.

All participants provided informed consent for the publication of their anonymised case details and images.

CRediT authorship contribution statement

Yuanyuan Zhang: Writing – original draft, Resources, Methodology, Investigation, Formal analysis, Data curation. **Weixue Jia:** Writing – original draft, Resources, Methodology, Formal analysis, Data curation. **Xue Wang:** Writing – original draft, Methodology, Formal analysis, Data curation. **Qiuxia Mao:** Writing – original draft, Methodology, Formal analysis, Data curation. **Lingling Luo:** Writing – original draft, Formal analysis, Data curation. **Lingzhuo Kong:** Formal analysis, Data curation. **Youming Guo:** Methodology, Formal analysis, Data curation. **Ran Mo:** Formal analysis, Data curation. **Wenbo Bu:** Writing – review & editing, Supervision, Resources, Project administration, Methodology, Funding acquisition, Formal analysis, Conceptualization. **Chengrang Li:** Writing – review & editing, Supervision, Project administration, Investigation, Funding acquisition, Formal analysis, Conceptualization.

Declaration of competing interest

The authors declare that they have no known competing financial interests or personal relationships that could have appeared to influence the work reported in this paper.

Appendix A. Supplementary data

Supplementary data to this article can be found online at https://doi.org/10.1016/j.heliyon.2024.e31509.

References

[1] B. Wang, W. Yang, W. Wen, et al., Gamma-secretase gene mutations in familial acne inversa, Science 330 (6007) (2010) 1065, https://doi.org/10.1126/science.1196284.

[2] J.W. Frew, D.A. Vekic, J. Woods, G.D. Cains, A systematic review and critical evaluation of reported pathogenic sequence variants in hidradenitis suppurativa, Br. J. Dermatol. 177 (4) (2017) 987–998, https://doi.org/10.1111/bjd.15441.

[3] Z.B. Ruan, X.L. Fu, W. Li, J. Ye, R.Z. Wang, L. Zhu, Effect of notch1,2,3 genes silicing on NF-κB signaling pathway of macrophages in patients with atherosclerosis, Biomed. Pharmacother. 84 (2016) 666–673, https://doi.org/10.1016/j.biopha.2016.09.078.

[4] W. Gao, C. Sweeney, C. Walsh, et al., Notch signalling pathways mediate synovial angiogenesis in response to vascular endothelial growth factor and angiopoietin 2, Ann. Rheum. Dis. 72 (6) (2013) 1080–1088, https://doi.org/10.1136/annrheumdis-2012-201978.

[5] X. Xiao, Y. He, C. Li, X. Zhang, H. Xu, B. Wang, Nicastrin mutations in familial acne inversa impact keratinocyte proliferation and differentiation through the Notch and phosphoinositide 3-kinase/AKT signalling pathways, Br. J. Dermatol. 174 (3) (2016) 522–532, https://doi.org/10.1111/bjd.14223.

[6] Y. He, H. Xu, C. Li, et al., Nicastrin/miR-30a-3p/RAB31 Axis regulates keratinocyte differentiation by impairing EGFR signaling in familial acne inversa, J. Invest. Dermatol. 139 (1) (2019) 124–134, https://doi.org/10.1016/j.jid.2018.07.020.

[7] V. De Vita, D. McGonagle, Hidradenitis suppurativa as an autoinflammatory keratinization disease, J. Allergy Clin. Immunol. 141 (5) (2018) 1953, https://doi.org/10.1016/j.jaci.2018.01.010.

[8] M. Von Laffert, P. Helmbold, J. Wohlrab, E. Fiedler, V. Stadie, W.C. Marsch, Hidradenitis suppurativa (acne inversa): early inflammatory events at terminal follicles and at interfollicular epidermis, Exp. Dermatol. 19 (6) (2010) 533–537, https://doi.org/10.1111/j.1600-0625.2009.00915.x.

[9] M. Von Laffert, V. Stadie, J. Wohlrab, W.C. Marsch, Hidradenitis suppurativa/acne inversa: bilocated epithelial hyperplasia with very different sequelae, Br. J. Dermatol. 164 (2) (2011) 367–371, https://doi.org/10.1111/j.1365-2133.2010.10034.x.

[10] T. Nomura, Hidradenitis suppurativa as a potential subtype of autoinflammatory keratinization disease, Front. Immunol. 11 (2020) 847, https://doi.org/10.3389/fimmu.2020.00847.

[11] Y. Tüzün, M. Antonov, N. Dolar, R. Wolf, Keratinocyte cytokine and chemokine receptors, Dermatol. Clin. 25 (4) (2007) 467–vii, https://doi.org/10.1016/j.det.2007.06.003.

[12] A.S. Byrd, C. Carmona-Rivera, L.J. O'Neil, et al., Neutrophil extracellular traps, B cells, and type I interferons contribute to immune dysregulation in hidradenitis suppurativa, Sci. Transl. Med. 11 (508) (2019) eaav5908.

[13] S. Li, S. Ying, Y. Wang, Y. Lv, J. Qiao, H. Fang, Neutrophil extracellular traps and neutrophilic dermatosis: an update review, Cell Death Dis. 10 (1) (2024) 18, https://doi.org/10.1038/s41420-023-01787-2. Published 2024 Jan 10.

[14] Y. Jiang, L.C. Tsoi, A.C. Billi, et al., Cytokinocytes: the diverse contribution of keratinocytes to immune responses in skin, JCI Insight 5 (20) (2020) e142067, https://doi.org/10.1172/jci.insight.142067.

[15] A.L. Lima, I. Karl, T. Giner, et al., Keratinocytes and neutrophils are important sources of proinflammatory molecules in hidradenitis suppurativa, Br. J. Dermatol. 174 (3) (2016) 514–521, https://doi.org/10.1111/bjd.14214.

[16] M.M. Lowe, H.B. Naik, S. Clancy, et al., Immunopathogenesis of hidradenitis suppurativa and response to anti-TNF-α therapy, JCI Insight 5 (19) (2020) e139932, https://doi.org/10.1172/jci.insight.139932.

[17] C. Gamell, A. Bankovacki, K. Scalzo-Inguanti, et al., CSL324, a granulocyte colony-stimulating factor receptor antagonist, blocks neutrophil migration markers that are upregulated in hidradenitis suppurativa, Br. J. Dermatol. 188 (5) (2023) 636–648, https://doi.org/10.1093/bjd/ljad013.

[18] J.L. Blok, K. Li, C. Brodmerkel, M.F. Jonkman, B. Horváth, Gene expression profiling of skin and blood in hidradenitis suppurativa, Br. J. Dermatol. 174 (6) (2016) 1392–1394, https://doi.org/10.1111/bjd.14371.

[19] S. Marrakchi, P. Guigue, B.R. Renshaw, et al., Interleukin-36-receptor antagonist deficiency and generalized pustular psoriasis, N. Engl. J. Med. 365 (7) (2011) 620–628, https://doi.org/10.1056/NEJMoa1013068.

[20] J.E. Towne, K.E. Garka, B.R. Renshaw, G.D. Virca, J.E. Sims, Interleukin (IL)-1F6, IL-1F8, and IL-1F9 signal through IL-1Rrp2 and IL-1RAcP to activate the pathway leading to NF-kappaB and MAPKs, J. Biol. Chem. 279 (14) (2004) 13677–13688, https://doi.org/10.1074/jbc.M400117200.

[21] J.E. Sims, D.E. Smith, The IL-1 family: regulators of immunity, Nat. Rev. Immunol. 10 (2) (2010) 89–102, https://doi.org/10.1038/nri2691.

[22] Y. Hayran, N. Allı, Ç. Yücel, N. Akdoğan, T. Turhan, Serum IL-36α, IL-36β, and IL-36γ levels in patients with hidradenitis suppurativa: association with disease characteristics, smoking, obesity, and metabolic syndrome, Arch. Dermatol. Res. 312 (3) (2020) 187–196, https://doi.org/10.1007/s00403-019-02012-w.

[23] G.P. Sullivan, C.M. Henry, D.M. Clancy, et al., Suppressing IL-36-driven inflammation using peptide pseudosubstrates for neutrophil proteases, Cell Death Dis. 9 (3) (2018) 378, https://doi.org/10.1038/s41419-018-0385-4. Published 2018 Mar 7.

[24] T.K. Satoh, M. Mellett, B. Meier-Schiesser, et al., IL-36γ drives skin toxicity induced by EGFR/MEK inhibition and commensal Cutibacterium acnes, J. Clin. Invest. 130 (3) (2020) 1417–1430, https://doi.org/10.1172/JCI128678.

[25] K.L. Sachen, C.N. Arnold Greving, J.E. Towne, Role of IL-36 cytokines in psoriasis and other inflammatory skin conditions, Cytokine 156 (2022) 155897, https://doi.org/10.1016/j.cyto.2022.155897.

[26] C.M. Henry, G.P. Sullivan, D.M. Clancy, I.S. Afonina, D. Kulms, S.J. Martin, Neutrophil-derived proteases escalate inflammation through activation of IL-36 family cytokines, Cell Rep. 14 (4) (2016) 708–722, https://doi.org/10.1016/j.celrep.2015.12.072.

[27] H.C. Ring, P. Riis Mikkelsen, I.M. Miller, et al., The bacteriology of hidradenitis suppurativa: a systematic review, Exp. Dermatol. 24 (10) (2015) 727–731, https://doi.org/10.1111/exd.12793.

[28] E.J. Giamarellos-Bourboulis, Staphylococcus aureus and host interaction in the flare-ups of hidradenitis suppurativa, Br. J. Dermatol. 181 (5) (2019) 892–893, https://doi.org/10.1111/bjd.18320.

[29] G. Nikolakis, O. Join-Lambert, I. Karagiannidis, H. Guet-Revillet, C.C. Zouboulis, A. Nassif, Bacteriology of hidradenitis suppurativa/acne inversa: a review, J. Am. Acad. Dermatol. 73 (5 Suppl 1) (2015) S12–S18, https://doi.org/10.1016/j.jaad.2015.07.041.

[30] S.R. Goldburg, B.E. Strober, M.J. Payette, Hidradenitis suppurativa: current and emerging treatments, J. Am. Acad. Dermatol. 82 (5) (2020) 1061–1082, https://doi.org/10.1016/j.jaad.2019.08.089.

[31] H.B. Naik, A. Nassif, M.S. Ramesh, et al., Are bacteria infectious pathogens in hidradenitis suppurativa? Debate at the symposium for hidradenitis suppurativa advances meeting, november 2017, J. Invest. Dermatol. 139 (1) (2019) 13–16, https://doi.org/10.1016/j.jid.2018.09.036.

[32] Y. Liu, S. Zhao, Y. Chen, et al., Vimentin promotes glioma progression and maintains glioma cell resistance to oxidative phosphorylation inhibition, Cell. Oncol. 46 (6) (2023) 1791–1806, https://doi.org/10.1007/s13402-023-00844-3.

[33] Y. Liu, Y. Chen, F. Wang, et al., Caveolin-1 promotes glioma progression and maintains its mitochondrial inhibition resistance, Discov Oncol 14 (1) (2023) 161, https://doi.org/10.1007/s12672-023-00765-5.

[34] Y. Chen, Y. Zhang, Z. Wang, et al., CHST15 gene germline mutation is associated with the development of familial myeloproliferative neoplasms and higher transformation risk, Cell Death Dis. 13 (7) (2022) 586, https://doi.org/10.1038/s41419-022-05035-w.

[35] J. Yang, L. Wang, Y. Huang, et al., Keratin 5-Cre-driven deletion of Ncstn in an acne inversa-like mouse model leads to a markedly increased IL-36a and Sprr2 expression, Front. Med. 14 (3) (2020) 305–317, https://doi.org/10.1007/s11684-019-0722-8.

[36] M. Tauber, E. Bal, X.Y. Pei, et al., IL36RN mutations affect protein expression and function: a basis for genotype-phenotype correlation in pustular diseases, J. Invest. Dermatol. 136 (9) (2016) 1811–1819, https://doi.org/10.1016/j.jid.2016.04.038.

[37] S. Hessam, M. Sand, T. Gambichler, M. Skrygan, I. Rüddel, F.G. Bechara, Interleukin-36 in hidradenitis suppurativa: evidence for a distinctive proinflammatory role and a key factor in the development of an inflammatory loop, Br. J. Dermatol. 178 (3) (2018) 761–767, https://doi.org/10.1111/bjd.16019.

[38] R. Thomi, M. Kakeda, N. Yawalkar, C. Schlapbach, R.E. Hunger, Increased expression of the interleukin-36 cytokines in lesions of hidradenitis suppurativa, J. Eur. Acad. Dermatol. Venereol. 31 (12) (2017) 2091–2096, https://doi.org/10.1111/jdv.14389.

[39] R. Di Caprio, A. Balato, G. Caiazzo, et al., IL-36 cytokines are increased in acne and hidradenitis suppurativa, Arch. Dermatol. Res. 309 (8) (2017) 673–678, https://doi.org/10.1007/s00403-017-1769-5.

[40] E. Scala, R. Di Caprio, S. Cacciapuoti, et al., A new T helper 17 cytokine in hidradenitis suppurativa: antimicrobial and proinflammatory role of interleukin-26, Br. J. Dermatol. 181 (5) (2019) 1038–1045, https://doi.org/10.1111/bjd.17854.
[41] K. Wolk, K. Warszawska, C. Hoeflich, et al., Deficiency of IL-22 contributes to a chronic inflammatory disease: pathogenetic mechanisms in acne inversa, J. Immunol. 186 (2) (2011) 1228–1239, https://doi.org/10.4049/jimmunol.0903907.
[42] G.L. Sen, L.D. Boxer, D.E. Webster, et al., ZNF750 is a p63 target gene that induces KLF4 to drive terminal epidermal differentiation, Dev. Cell 22 (3) (2012) 669–677, https://doi.org/10.1016/j.devcel.2011.12.001.
[43] L. Jin, Y. Chen, S. Muzaffar, et al., Epigenetic switch reshapes epithelial progenitor cell signatures and drives inflammatory pathogenesis in hidradenitis suppurativa, Proc. Natl. Acad. Sci. U. S. A. 120 (49) (2023) e2315096120, https://doi.org/10.1073/pnas.2315096120.
[44] A. Johnston, X. Xing, L. Wolterink, et al., IL-1 and IL-36 are dominant cytokines in generalized pustular psoriasis, J. Allergy Clin. Immunol. 140 (1) (2017) 109–120, https://doi.org/10.1016/j.jaci.2016.08.056.
[45] J.S. Ainscough, T. Macleod, D. McGonagle, et al., Cathepsin S is the major activator of the psoriasis-associated proinflammatory cytokine IL-36γ, Proc. Natl. Acad. Sci. U. S. A. 114 (13) (2017) E2748–E2757, https://doi.org/10.1073/pnas.1620954114.
[46] O. Vasiljeva, M. Dolinar, J.R. Pungercar, V. Turk, B. Turk, Recombinant human procathepsin S is capable of autocatalytic processing at neutral pH in the presence of glycosaminoglycans, FEBS Lett. 579 (5) (2005) 1285–1290, https://doi.org/10.1016/j.febslet.2004.12.093.
[47] K.T. Savage, M.R. Santillan, K.S. Flood, A. Charrow, M.L. Porter, A.B. Kimball, Tofacitinib shows benefit in conjunction with other therapies in recalcitrant hidradenitis suppurativa patients, JAAD Case Rep 6 (2) (2020) 99–102, https://doi.org/10.1016/j.jdcr.2019.10.010.
[48] K. Storm van's Gravesande, M.D. Layne, Q. Ye, et al., IFN regulatory factor-1 regulates IFN-gamma-dependent cathepsin S expression, J. Immunol. 168 (9) (2002) 4488–4494, https://doi.org/10.4049/jimmunol.168.9.4488.
[49] V.K. Shanmugam, D. Jones, S. McNish, M.L. Bendall, K.A. Crandall, Transcriptome patterns in hidradenitis suppurativa: support for the role of antimicrobial peptides and interferon pathways in disease pathogenesis, Clin. Exp. Dermatol. 44 (8) (2019) 882–892, https://doi.org/10.1111/ced.13959.
[50] C. Hotz, M. Boniotto, A. Guguin, et al., Intrinsic defect in keratinocyte function leads to inflammation in hidradenitis suppurativa, J. Invest. Dermatol. 136 (9) (2016) 1768–1780, https://doi.org/10.1016/j.jid.2016.04.036.
[51] H. Guet-Revillet, H. Coignard-Biehler, J.P. Jais, et al., Bacterial pathogens associated with hidradenitis suppurativa, France, Emerg. Infect. Dis. 20 (12) (2014) 1990–1998, https://doi.org/10.3201/eid2012.140064.
[52] U. Mrowietz, A.D. Burden, A. Pinter, et al., Spesolimab, an anti-interleukin-36 receptor antibody, in patients with palmoplantar pustulosis: results of a phase IIa, multicenter, double-blind, randomized, placebo-controlled pilot study, Dermatol. Ther. 11 (2) (2021) 571–585, https://doi.org/10.1007/s13555-021-00504-0.
[53] S.E. Choon, M.G. Lebwohl, S. Marrakchi, et al., Study protocol of the global Effisayil 1 Phase II, multicentre, randomised, double-blind, placebo-controlled trial of spesolimab in patients with generalized pustular psoriasis presenting with an acute flare, BMJ Open 11 (3) (2021) e043666, https://doi.org/10.1136/bmjopen-2020-043666.